Self-consistent thermal model of semiconductor disk lasers

Ł. BIELARCZYK, W. NAKWASKI*, R. P. SARZAŁA
Photonics Group, Institute of Physics, Technical University of Lodz
ul. Wolczanska 219, 90-924 Lodz, Poland

Self-consistent thermal model of semiconductor disk lasers is presented. The model was used to study thermal properties of the GaAs-based InGaAs/GaAs quantum-well disk laser emitting the 980-nm radiation and equipped with a heat spreader. For a proper laser thermal management, the 300-μm CVD heat spreader has been found to be optimal, an optimal diameter of the pumping spot is equal to about 200 μm and optimal radii of the laser copper heat sink and the laser crystal are equal to about 7.5 mm and 2.5 mm, respectively.

(Received December 20, 2010; accepted January 26, 2011)

Keywords: Semiconductor disk laser, Vertical external-cavity surface-emitting laser (VECSEL), Thermal VECSEL model

1. Introduction

There are two basic configurations of electrically-pumped diode lasers: edge-emitting lasers (EELs) and vertical-cavity surface-emitting lasers (VCSELs). Single EEL can emit even tens of watts of output power but its radiation contains then many modes and its output beam is asymmetric and considerably divergent. In contrast, VCSELs offer a single-mode, circularly symmetric, low-divergent output beam, but only for relatively low output of several milliwatts. New optically pumped semiconductor disk lasers, known also as vertical external-cavity surface-emitting lasers (VECSELs) [1,2], have been created to combine simultaneously virtues of both the above diode lasers, i.e. to obtain a device emitting a high-quality output beam of watt-level.

Thermal problems, as practically in all high-power devices, especially during their infant period, are currently the most important ones limiting possible VESCSEL applications. As much as about 70% of the optical pumping power is believed in these devices to be exchanged into heat. Besides, relatively high temperature increases within their volumes result from the fact, that the heat flux generated mainly within the VECSEL active region has to flow through the low-thermal-conductivity multi-layer distributed Bragg reflector (DBR) and the thick substrate. Assuming 100 μm x 100 μm pump spot and a simplified one-dimensional heat flow (confirmed by our calculations) through the GaAs substrate, each micrometer of its thickness results in about 2.2 K/W thermal impedance [3].

From among various physical phenomena enhanced by a temperature increase within a VECSEL volume, a decreasing maximal optical gain in active-region quantum wells (QWs), an increasing thermal escape of carriers from them additionally reducing an optical gain, temperature-dependent both thermal conductivities and absorption as well as detuning of an standing optical wave with QW positions (because of a temperature dependence of refractive indices n_R) deteriorating efficiency of its resonant-periodic-gain (RPG) structure, are the most significant ones. Therefore the main aim of this paper is to propose a detailed self-consistent model of thermal properties of semiconductor disk lasers which may enable their thermal optimization, i.e. an improvement of an efficiency of a heat-flux extraction from their cavities. Similar, but somewhat more simplified model has been also reported by Kemp et al. [4].

2. Structure of a semiconductor disk laser

Let us consider a semiconductor crystal of radius r_S = 2.5 mm of a typical optically-pumped disk laser [5] (shown schematically in Fig. 1) with the upper heat spreader transparent for both the pump and the emitted radiation. The high-conductivity (SiC or diamond) heat spreader of the 300-μm thickness is bonded directly on the laser crystal using liquid capillarity [6] to improve heat extraction from it, which means – to enhance a radial heat-flux spreading increasing the width of its heat path towards the heat-sink of the r_{HS} = 7.5 mm radius. The disk laser is assumed to emit the λ = 980-nm radiation and to be pumped by the 808-nm radiation. A relatively small energy difference between the pump and the emitted radiation is intentionally applied because heat generation is proportional to it [4,7]. The pumping beam is directed at some angle with respect to the laser axis through the upper window, through which also the output beam is emitted in axial direction. An external spherical mirror (not shown in Fig. 1) is used to create a laser cavity with the semiconductor DBR.

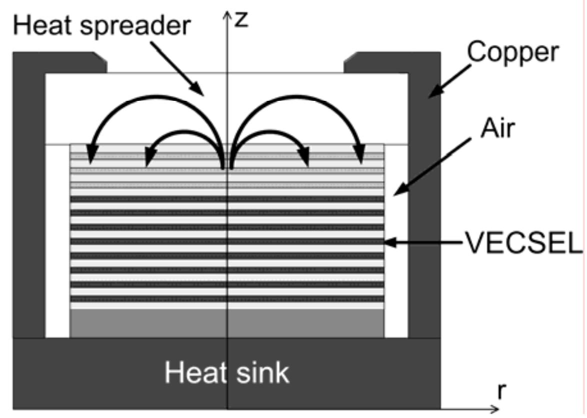

Fig. 1 Schematic structure of a semiconductor crystal of an optically-pumped semiconductor disk laser with an upper heat spreader. The 0rz co-ordinate system is shown

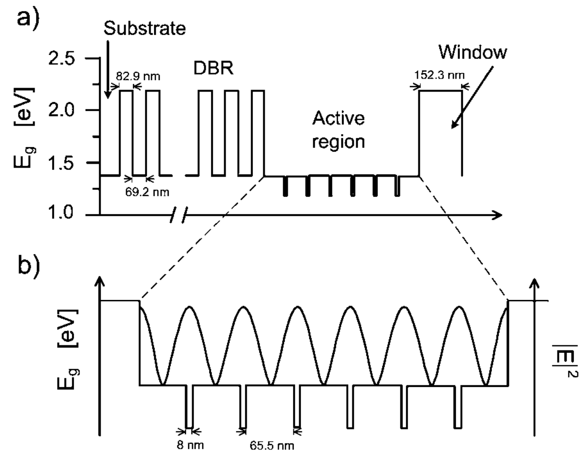

Fig. 2 VECSEL layers

More information about the layered VECSEL structure under consideration, which was manufactured by the Institute of Electron Technology in Warsaw [8], may be found in Fig. 2. The laser is produced in a single technological process on the 80-μm GaAs substrate. All epitaxial layers are un-doped to reduce radiation losses due to free-carrier absorption. First the 27-period DBR formed by the alternative 69.2-nm GaAs and 82.9-nm AlAs layers is created. Next the active region composed of six the 8-nm InGaAs QWs separated by the 65.5-nm (= $\lambda/2n_{R,GaAs}$) GaAs barriers is deposited to create the RPG arrangement, i.e. with QWs located at the successive anti-node positions of the optical standing wave. To supply the active region with carriers, the barrier pumping system is used, which means, that the pumping beam is mostly absorbed inside the barrier layers surrounding QWs. Expected short absorption lengths (1 – 2 μm) [3] results in efficient pump absorption. Then some of the excited carriers are injected into QWs where they mostly recombine radiatively. And finally, the 152.3-nm (= $\lambda/2n_{R,AlGaAs}$) $Al_{0.5}Ga_{0.5}As$ window layer transparent for the pumping beam is produced and covered with the thin cap GaAs layer to protect it against the air oxidation. The window layer prevents the carriers from their non-radiative recombination on the surface [9]. The pumping beam is absorbed in GaAs layers of both the active region and the DBR structure, which is highly reflective for the VECSEL radiation but not for the pumping one. The laser structure is bonded to the 15-mm copper heat sink with the aid of the 4-μm indium solder.

3. Model

Following its name, the semiconductor disk laser is assumed to be cylindrically symmetric (Fig. 1). Temperature profiles $T(r,z)$ within its volume may be determined with the aid of the thermal conduction equation:

$$\frac{1}{r}\frac{\partial}{\partial r}\left[k(r,z,T)\frac{\partial T}{\partial r}\right]+\frac{\partial}{\partial z}\left[k(r,z,T)\frac{\partial T}{\partial z}\right]+g_T(r,z)=0 \quad (1)$$

where k stands for a thermal conductivity and g_T is a volume density of heat sources. As one can see, thermal conductivities are assumed to be dependent on temperature therefore the self-consistent method of calculations is applied. Heat extraction through the bottom heat sink is so efficient that the upper and the side walls of the laser crystal may be assumed to be thermally isolated:

$$\frac{\partial T}{\partial r}(r=r_S)=\frac{\partial T}{\partial z}(z=z_T)=0 \quad (2)$$

where z_T stands for the height of the laser crystal. Sizes of the copper heat sink are much larger than those of the laser crystal, therefore the bottom and the side walls of the heat sink are assumed to be kept at the ambient temperature T_A. Besides, because of the cylindrical symmetry:

$$\frac{\partial T}{\partial r}(r=0)=0 \quad (3)$$

Assuming Gaussian spatial profile of the pumping beam, the analogous (but dependent also on the z location) profile may be assumed for the volume density of heat sources being a result of its absorption:

$$g_T(r,z) = g_{T,0}(z)\exp\left(-\frac{r^2}{2\sigma^2}\right) \tag{4}$$

where σ stands for the distribution parameter. The above central (for $r = 0$) heat-generation density $g_{T,0}$ in successive structure layers depends on local absorption coefficients and on a pumping intensity being gradually reduced by this absorption. Absorption coefficients within the GaAs layers (active-region barriers, DBR and substrate) and within the InGaAs QWs are assumed to be equal to 20 000 cm^{-1} and 15 000 cm^{-1}, respectively. It should also be noted, that a uniform (not Gaussian) pumping distribution could lead to lower temperature increases within the pumped crystal [10].

Thermal conductivities at room temperature (T_A = 300 K) of the $In_xGa_{1-x}As$ [11] and the $Al_xGa_{1-x}As$ [12] layers are given in the following forms:

$$k_{InGaAs} = \frac{100}{2.27 + 80.23x - 78.80x^2}\left[\frac{W}{mK}\right] \tag{5}$$

$$k_{AlGaAs} = \frac{100}{2.27 + 28.83x - 30.00x^2}\left[\frac{W}{mK}\right] \tag{6}$$

whereas, at higher temperatures T, they are assumed to be proportional to $(T_A/T)^{5/4}$ [12]. Thermal conductivities of indium, k_{In} = 81.6 W/mK [13], copper, k_{Cu} = 401 W/mK [14], SiC, k_{SiC} = 490 W/mK [15] and synthetic CVD diamond, k_{CVD} = 1200 W/mK [16], are assumed to be independent of temperature.

Temperature profiles within a volume of the semiconductor disk laser are determined with the aid of the finite-element self-consistent approach [17,18], which is finished when temperature profiles determined in two successive iteration loops become practically unchanged. Mesh sizes in various structure areas are properly changed to achieve an expected exactness while simultaneously to reduce the number of elements.

Similar model has been also reported by Kemp et al. [4,19], but their VECSEL structure has been somewhat different. Moreover, instead of thermal conductivities of successive structure layers as in our model, effective conductivities [20] determined for some layer groups have been used. It considerably reduces calculation time but, at the same time, it may considerably influence model exactness, especially in the case of large conductivity changes between adjacent layers, as it is in the GaAs/AlAs DBR. Furthermore, temperature dependence of thermal conductivities is neglected in their model which may have serious impact on model exactness for relatively high temperature increases. Besides, their model neglects heat-flux spreading within the heat sink. Thermal model of a still another VECSEL structure without a heat spreader but with a substrate intentionally substantially thinned has been reported in [21].

4. Results

The VECSEL crystal under consideration is assumed to be kept at 300 K and to be pumped by the 808-nm 4-W Gaussian laser beam of the distribution parameter σ = 50 μm, which corresponds to ϕ = 4σ = 200 μm beam diameter. Most of absorption of the pumping radiation leads to an intense heat generation followed by an increase in temperature which for the considered device should not exceed 400 K because of possible problems with the indium solder. Besides temperature increases deteriorate device performance, in particular, they may lead to an accelerated device catastrophic degradation. The heat spreader is bonded directly on the laser crystal using liquid capillarity. Possible imperfection of this connection may result in a huge temperature increase because the air thermal conductivity (0.025 W/mK) is extremely low. But, assuming its nearly perfect properties, in the calculation, a reasonable thermal resistance of 3 K/W for this bonding is assumed.

Two different heat spreaders made of SiC and CVD have been used. Axial temperature profiles along the direction perpendicular to layer boundaries, are shown for both of them in Fig. 3. As expected, temperature increase is the highest within the active region and is practically confined to its close surrounding. Besides, maximal temperature increase is distinctly higher (43.8 K versus 28.6 K) in the case, when the lower-thermal-conductivity SiC heat spreader is used instead of the CVD one, which confirms significance of its conductivity. For pumping powers lower than 4 W, maximal active-region temperature T_{max} depends linearly on them in disk lasers with both heat spreaders, which was confirmed experimentally [7]. As one can see in Fig. 3 comparing slopes of temperature profiles on both sides of the active-region temperature peak, both heat fluxes flowing from the active region, i.e. the first one directly towards the heat sink and the second one as a result of its radial spreading within the heat spreader, are of comparable intensity, although surprisingly the second flux is somewhat more intense. The temperature slope towards the heat sink is nearly linear, which confirms its nearly one-dimensional nature, whereas the one in the opposite direction is distinctly curved, which is typical for a two-dimensional heat-flux spreading. Radial temperature profiles within the active region are plotted in Fig. 4. Intensity of the radial heat fluxes are similar in both the cases. It is also shown that the radius of the central higher-temperature active-region area is equal to about 100 μm.

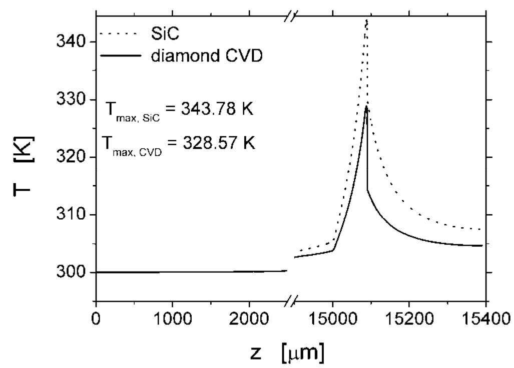

Fig. 3 Axial temperature profiles along the direction perpendicular to layer boundaries determined for the disk laser pumped by the 4-W radiation. The SiC and the CVD heat spreaders are considered. Maximal temperature increases are given.

It is evident from Fig. 3 and Fig. 4, that the thermal conductivity of a heat spreader is in this case of prime importance. Fig. 5 presents a dependence on the heat-spreader thermal conductivity k_{hs} of the maximal temperature T_{max} within the active region for the heat-spreader of the nominal thickness d_{hs} = 300 μm. As expected, T_{max} increases considerably with a decrease in k_{hs}, which confirms importance of a heat-spreader quality. Besides, effectiveness of heat-flux spreading depends also on the heat-spreader thickness d_{hs}, which is illustrated in Fig. 6. As one can see, an increase in d_{hs} over its nominal value of 300 μm does not lead to a significant improvement of heat-flux spreading, whereas its decrease below this value may result in its serious deterioration. If the heat spreader is completely removed, the maximal active-region temperature T_{max} = 381 K may be expected. Besides, a temperature increase within the active region depends also on a diameter ϕ of the pumping beam, which is shown in Fig. 7. Again, while a reduction of ϕ below its nominal value of 200 μm leads to an unwanted active-region temperature increase, its further increase has a significantly less impact. For ϕ changed from 300 μm to only 100 μm, T_{max} is reduced by as much as 87 K for the SiC heat spreader and by 62 K – for the CVD one. The above optimal ϕ value of 200 μm has been determined for the considered VECSEL structure and the Gaussian pumping beam to maintain low enough the active-region temperature. Generally, increasing pump area results in both higher output power and more efficient heat-flux extraction from the laser volume [22].

It is clearly seen in the above figures, that, although a dominant contribution to the VECSEL thermal resistance comes from its DBR, the thick substrate also causes a serious temperature increase within the laser active region. Hence sometimes, instead of using the upper heat spreader, thinning of the substrate (e.g. [3,23,24]) is used to enhance heat-flux extraction from a volume of disk lasers.

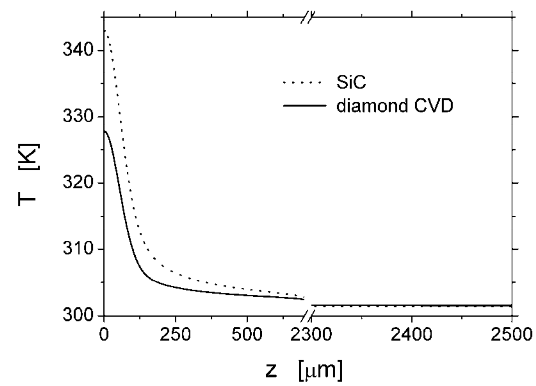

Fig. 4 Radial temperature profiles determined for the active layer of the disk laser pumped by the 4-W radiation. The SiC and the CVD heat spreaders are considered.

For the considered disk laser with the SiC heat spreader, an impact on T_{max} of the substrate thickness d_{sub} is shown in Fig. 8. As one can see, a complete substrate removing leads in this laser to a decrease in T_{max} from about 344 K to only 330 K. Substrate thinning is especially effective in lasers with upper heat spreaders of relatively low thermal conductivities, therefore this method is practically useless in lasers with diamond heat spreaders. Also sizes of the copper heat sink may have quite a serious impact on temperature increases within the disk laser. It was found that, for the disk laser with the SiC heat spreader, a decrease in the heat-sink radius r_{HS} from its nominal value of 7.5 mm to only 2.5 mm equal to the radius r_S of the disk laser results in about 6 K increase in the maximal active-region temperature.

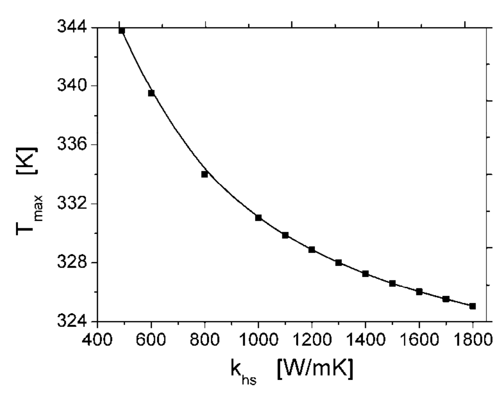

Fig. 5 Maximal active-region temperature T_{max} versus the thermal conductivity k_{hs} of the heat spreader of the nominal thickness d_{hs} = 300 μm.

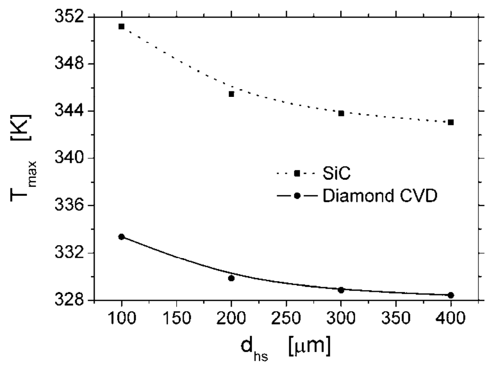

Fig. 6 Maximal active-region temperature T_{max} versus a thickness d_{hs} of the SiC and CVD heat spreaders.

An increase in r_{HS} over 7.5 mm does not influence heat extraction from the disk laser. An increase in the radius r_S of the disk laser over its nominal value of 2.5 mm completely does not lead to any improvement of the above heat extraction but its reduction below this value may considerably deteriorate it and, for r_{HS} = 0.5 mm, T_{max} is increased in disk lasers with the SiC heat spreader by 9 K. r_{HS} = 2.5 mm was also found as an optimal value by other authors [25].

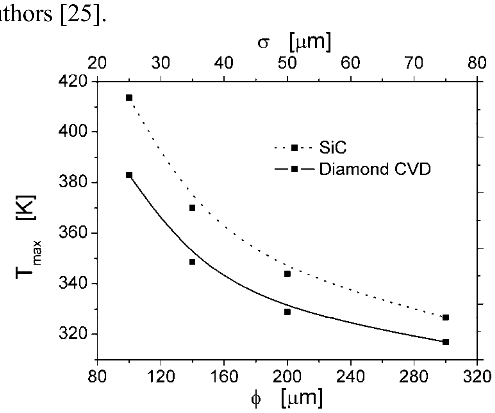

Fig. 7 Maximal active-region temperature T_{max} versus a diameter ϕ of the pumping beam for disk lasers with nominal SiC and CVD heat spreaders.

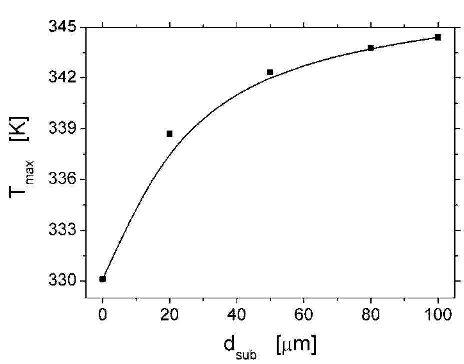

Fig. 8 Maximal active-region temperature T_{max} versus the substrate thickness d_{sub} for disk lasers with the nominal SiC heat spreader.

5. Conclusions

The self-consistent thermal model of a disk laser was prepared to study thermal properties of the GaAs-based laser emitting the 980-nm radiation and equipped with six InGaAs quantum wells separated by GaAs barriers to form the resonant-periodic-gain structure, the 80-μm GaAs substrate, the 27-period GaAs/AlAs distributed Bragg mirrors, the λ/2 window layer and the 300-μm SiC or CVD heat spreader. As expected, heat-spreader thermal conductivity is of prime importance in thermal laser management, hence the CVD heat spreader offers much better performance than the SiC one. For the VECSEL structure under consideration, the optimal heat-spreader thickness has been found to be equal to about 300 μm, the optimal diameter of the pumping spot is equal to about 200 μm and the optimal radii of the laser copper heat sink and the laser crystal are equal to about 7.5 mm and 2.5 mm, respectively.

Acknowledgement

This work has been supported by the COST Action MP0805 and by the Polish Ministry of Science and Higher Education (MNiSzW), grant No NN 515 417 635.

References

[1] O. G. Okhotnikov (Ed.), Semiconductor Disk Lasers, Wiley-VCH, Weinheim (2010).
[2] S. Calvez, J. E. Hastie, M. Guina, O. G. Okhotnikov, M. D. Dawson, Laser & Photon. Rev., **3**, 407 (2009).
[3] M. Kuznetsov, F. Hakimi, R. Sprague, A. Mooradian, IEEE J. Select. Topics Quantum Electron. **5**, 561 (1999).
[4] A. J. Kemp, G. J. Valentine, J. M. Hopkins, J. E. Hastie, S. A. Smith, S. Calvez, M. D. Dawson, D. Burns, IEEE J. Quantum Electron. **41**, 148 (2005).
[5] J. E. Hastie, J. M. Hopkins, S. Calvez, C. W. Jeon, D. Burns, R. Abram, E. Riis, A. I. Ferguson, M. D. Dawson, IEEE Photn. Techn. Lett. **15**, 894 (2003).
[6] Z. L. Liau, Appl. Phys. Lett. **77**, 651 (2000).
[7] K. Pierściński, D. Pierścińska, M. Bugajski, C. Manz, M. Rattunde, Microel. J., **40**, 558 (2009).
[8] A. Wójcik-Jedlińska, K. Pierściński, A. Jasik, J. Muszalski, M. Bugajski, Opt. Appl., **37**, 499 (2007).
[9] B. Rösener, N. Schulz, M. Rattunde, C. Manz, K. Köhler, IEEE Photon. Techn. Lett., **20**, 1041 (2008).
[10] J. Brand, S. George, Surf. Sci., **167**, 341 (1986).
[11] W. Nakwaski, J. Appl. Phys., **64**, 159 (1988).
[12] A. Amith, I. Kudman, E. F. Steigmeier, Phys. Rev., **138**, A1270 (1965).
[13] Y. S. Touloukian, R. W. Powell, C. Y. Ho, P. G. Klemens, Thermophysical Properties of Matter, Plenum, New York (1970).
[14] D. R. Linde, CRC Handbook of Chemistry and Physics, CRC Press (2005).

[15] A. C. Tropper, S. H. Hoogland, Prog. Quantum Electron., **30**, 1 (2006).
[16] U. Keller, A. C. Tropper, Phys. Reports, No **429**, 67 (2006).
[17] Zienkiewicz O.C., Taylor R.L.: The finite element method, T. 1-3, Butterworth Heinemann, Oxford, 2000.
[18] Ł. Piskorski, R. P. Sarzała, M. Wasiak, W. Nakwaski, Opto-Electron. Review, **17**, 40 (2009).
[19] S. Calvez, J. E. Hastie, A. J. Kemp, [Chapter 2 in] O. G. Okhotnikov (Ed.), Semiconductor Disk Lasers, Wiley-VCH, Weinheim (2010).
[20] M. Osiński, W. Nakwaski, Electron. Lett. **29**, 1015 (1993).
[21] A. R. Zakharian, J. Hader, J. V. Moloney, S. W. Koch, P. Brick, S. Lutgen, Appl. Phys. Lett., **83**, 1313 (2003).
[22] M. Kuznetsov, [Chapter 1 in] O. G. Okhotnikov (Ed.), Semiconductor Disk Lasers, Wiley-VCH, Weinheim (2010).
[23] R. Häring, R. Paschotta, A. Aschwanden, E. Gini, F. Morier-Genoud, U. Keller, IEEE J. Quantum Electron., **38**, 1268 (2002).
[24] A. R. Zakharian, J. Hader, J. V. Moloney, S. W. Koch, P. Brick, S. Lutgen, Appl. Phys. Lett. **83**, 1313 (2003).
[25] M. Wasiak, R. P. Sarzała, A. Jasik, ICTON 2009, 11th Intern. Conference on Transparent Optical Networks.

*Corresponding author: nakwaski@p.lodz.pl